Calculation of the enrichment of the giant planet envelopes during the "late heavy bombardment"

Alexis Matter, Tristan Guillot, Alessandro Morbidelli

Calculation of the enrichment of the giant planets envelopes during the "late heavy bombardment"

A. Matter [a,*] T. Guillot [b] A. Morbidelli [c]

[a] *Laboratoire Fizeau, CNRS UMR 6203, Observatoire de la Côte d'Azur, BP 4229, 06304 Nice Cedex 4, France. Phone: +33 (0)4 92 00 30 68, fax: +33 (0)4 92 00 31 38*

[b] *Laboratoire Cassiopée, CNRS UMR 6202, Observatoire de la Côte d'Azur, BP 4229, 06304 Nice Cedex 4, France. Phone: +33 (0)4 92 00 30 47, fax: +33 (0)4 92 00 31 21*

[c] *Laboratoire Cassiopée, CNRS UMR 6202, Observatoire de la Côte d'Azur, BP 4229, 06304 Nice Cedex 4, France. Phone: +33 (0)4 92 00 31 26, fax: +33 (0)4 92 00 31 21*

Abstract

The giant planets of our solar system possess envelopes consisting mainly of hydrogen and helium but are also significantly enriched in heavier elements relatively to our Sun. In order to better constrain how these heavy elements have been delivered, we quantify the amount accreted during the so-called "late heavy bombardment", at a time when planets were fully formed and planetesimals could not sink deep into the planets. On the basis of the "Nice model", we obtain accreted masses (in terrestrial units) equal to $0.15 \pm 0.04\,M_\oplus$ for Jupiter, and $0.08 \pm 0.01\,M_\oplus$ for Saturn. For the two other giant planets, the results are found to depend mostly on whether

they switched position during the instability phase. For Uranus, the accreted mass is $0.051 \pm 0.003\,M_\oplus$ with an inversion and $0.030 \pm 0.001\,M_\oplus$ without an inversion. Neptune accretes $0.048 \pm 0.015\,M_\oplus$ in models in which it is initially closer to the Sun than Uranus, and $0.066 \pm 0.006\,M_\oplus$ otherwise. With well-mixed envelopes, this corresponds to an increase in the enrichment over the solar value of 0.033 ± 0.001 and 0.074 ± 0.007 for Jupiter and Saturn, respectively. For the two other planets, we find the enrichments to be 2.1 ± 1.4 (w/ inversion) or 1.2 ± 0.7 (w/o inversion) for Uranus, and 2.0 ± 1.2 (w/ inversion) or 2.7 ± 1.6 (w/o inversion) for Neptune. This is clearly insufficient to explain the inferred enrichments of ~ 4 for Jupiter, ~ 7 for Saturn and ~ 45 for Uranus and Neptune.

Key words: giant planets, planet formation, Jupiter, Saturn, Uranus, Neptune

1 Introduction

The four giant planets of our solar system have hydrogen and helium envelopes which are enriched in heavy elements with respect to the solar composition. In Jupiter, for which precise measurements from the Galileo probe are available, C, N, S, Ar, Kr, Xe are all found to be enriched compared to the solar value by factors 2 to 4 (Owen et al., 1999; Wong et al., 2004) (Assuming solar abundances based on the compilation by Lodders (2003)). In Saturn, the C/H ratio is found to be 7.4 ± 1.7 times solar (Flasar et al., 2005). In Uranus and Neptune it is approximately 45 ± 20 times solar (Guillot and Gautier, 2007)

* Corresponding author.
Email addresses: Alexis.Matter@obs-nice.fr (A. Matter),
Tristan.Guillot@obs-nice.fr (T. Guillot),
Alessandro.Morbidelli@obs-nice.fr (A. Morbidelli).

(corresponding to about 30 times solar with the old solar abundances). Interior models fitting the measured gravitational fields constrain enrichments to be between 1.5 and 8 for Jupiter and between 1.5 and 7 times the solar value for Saturn (Saumon and Guillot, 2004). For Uranus and Neptune, the envelopes are not massive enough (1 to 4 Earth masses) for interior models to provide global constraints on their compositions.

Enriching giant planets in heavy elements is not straightforward. Guillot and Gladman (2000) have shown that once the planets have their final masses, the ability of Jupiter to eject planetesimals severely limits the fraction that can be accreted by any planet in the system. The explanations put forward then generally imply an early enrichment mechanism:

- Alibert et al. (2005) show that migrating protoplanets can have access to a relatively large reservoir of planetesimals and accrete them in an early phase before they have reached their final masses and started their contraction. This requires the elements to be mixed upward efficiently, which is energetically possible, and may even lead to an erosion of Jupiter's central core (Guillot et al., 2004).
- The forming giant planets may accrete a gas that has been enriched in heavy elements through the photoevaporation of the protoplanetary disk's atmosphere, mainly made of hydrogen and helium (Guillot and Hueso, 2006). This could explain the budget in noble gases seen in Jupiter's atmosphere but is not sufficient to explain the enrichment in elements such as C, N, O because small grains are prevented from reaching the planet due to the formation of a dust-free gap (eg. Paardekooper, 2007). The photoevaporation model requires that the giant planets form late in the evolution of

disks, which appears consistent with modern scenarios of planet formation (see Ida and Lin (2004); Ida et al. (2008)). It also implies that a significant amount of solids are retained in the disk up to these late stages, as plausible from simulations of disk evolution (e.g. Garaud (2007)).

It has been recently suggested that the Solar System underwent a major change of structure during the phase called 'Late Heavy Bombardment' (LHB) (Tsiganis et al., 2005; Gomes et al., 2005). This phase, which occurred $\sim$ 650 My after planet formation, was characterized by a spike in the cratering history of the terrestrial planets.

The model that describes these structural changes, often called the 'Nice model' because it was developed in the city of Nice, reproduces most of the current orbital characteristics of both planets and small bodies. This model provides relatively tight constraints on both the location of the planets and on the position and mass of the planetesimal disk at the time of the disappearance of the proto-planetary nebula. Thus, it is interesting to study the amount of mass accreted by the planets at the time of the LHB, in the framework of this model.

The article is organized as follows: we first describe the orbital evolution model at the base of the calculation. Physical radii of the giant planets at the time of the late heavy bombardment are also discussed. We then present results, both in terms of a global enrichment and in the unlikely case of an imperfect mixing of the giant planets envelopes.

2 The 'Nice' model of the LHB

2.1 General description

The Nice model postulates that the ratio of the orbital periods of Saturn and Jupiter was initially slightly less than 2, so that the planets were close to their mutual 1:2 mean motion resonance (MMR); Uranus and Neptune were supposedly orbiting the Sun a few AUs beyond the gas giants, and a massive planetesimal disk was extending from 15.5 AU, that is about 1.5 AU beyond the last planet, up to 30–35 AU.

As a consequence of the interaction of the planets with the planetesimal disk, the giant planets suffered orbital migration, which slowly increased their orbital separation. As shown in Gomes et al. (2005) N-body simulations, after a long quiescent phase (with a duration varying from 300 My to 1 Gy, depending on the exact initial conditions), Jupiter and Saturn were forced to cross their mutual 1:2 MMR. This event excited their orbital eccentricities to values similar to those presently observed.

The acquisition of eccentricity by both gas giants destabilized Uranus and Neptune. Their orbits became very eccentric, so that they penetrated deep into the planetesimal disk. Thus, the planetesimal disk was dispersed, and the interaction between planets and planetesimals finally parked all four planets on orbits with separations, eccentricities and inclinations similar to what we currently observe.

This model has a long list of successes. It explains the current orbital architecture of the giant planets (Tsiganis et al., 2005). It also explains the origin and the properties of the LHB. In the Nice model, the LHB is triggered by

the dispersion of the planetesimal disk; both the timing, the duration and the intensity of the LHB deduced from Lunar constraints are well reproduced by the model (Gomes et al., 2005).

Furthermore, the Nice model also explains the capture of planetesimals around the Lagrangian points of Jupiter, with a total mass and orbital distribution consistent with the observed Jupiter Trojans (Morbidelli et al., 2005). More recently, it has been shown to provide a framework for understanding the capture and orbital distribution of the irregular satellites of Saturn, Uranus and Neptune, but not of Jupiter (Nesvorný et al., 2007), except in the case of an encounter between Jupiter and Neptune which is a rare but not impossible event. The main properties of the Kuiper belt (the relic of the primitive trans-planetary planetesimal disk) have also been explained in the context of the Nice model (Levison et al. (2008); see Morbidelli et al. (2008), for a review).

2.2 The dynamical simulations

In this work, we use 5 of the numerical simulations performed in (Gomes et al., 2005). The main simulation is the one illustrated in the figures of the Gomes et al. paper. The 1:2 MMR crossing between Jupiter and Saturn occurs after 880 My, relatively close to the observed timing of the LHB (650 My). When the instability occurs, the disk of planetesimals still contained 24 of its initial 35 Earth masses ($M_\oplus$).

During the evolution that followed the resonance crossing, Uranus and Neptune switched position. Thus, according to this simulation, the planet that ended up at $\sim$ 30 AU (Neptune) had to form closer to the Sun than the planet that reached a final orbit at $\sim$ 20 AU (Uranus).

However, because the planets evolutions are chaotic during the instability phase, different outcomes can be possible. Thus Gomes et al. performed 4 additional simulations with initial conditions taken from the state of the system in the main simulation just before the 1:2 resonance crossing, with slight changes in the planets' velocities. Two of these 'cloned' simulations again showed a switch in positions between Uranus and Neptune, but the two others did not. That is, in these two cases the planet that terminated its evolution at 30 AU also started the furthest from the Sun.

Here we use these 5 simulations (the main one and its 4 'clones') to evaluate the amount of solid material accreted by the planets and how it could vary depending on the specific evolutions of the ice giants. Notice that, whereas the main simulation spans 1.2 Gy (and therefore continues for 320 My after the 1:2 MMR crossing), the cloned simulations cover only a time-span of approximately 20 My, and were stopped when the planets reached well separated, relatively stable orbits.

2.3 Probability of impact and accretion of planetesimals

From these dynamical simulations, several steps are necessary to estimate the amount of mass accreted by the planets.

For each simulation at each output time (every 1 My) we have the orbital elements of the planets and of all the planetesimals in the system. We are aware that this time interval may be a bit too long to resolve the evolution of the system during the transient phases that immediately follow the onset of the planetary instability. On the other hand, when the instability occurs, most of the disk is still located beyond the orbits of the planet, so that the

bombardment rate is not very high. Thus, we believe that this coarse time sampling is enough for our purposes.

First we look for planetesimals that are in a mean motion resonance with a planet. The resonances taken into account are the 1:1, 1:2, 2:3, 2:1, 3:2. When computing the collision probability with a planet, the objects in resonance with that planet will not be taken into account (but they will be considered for the collision probability with the other planets). The rationale for this is that the resonant objects, even if planet-crosser, cannot collide with the planet, because they are phase-protected by the resonant configuration, as in the case of Pluto.

The width of a resonance is proportionnal to $\sqrt{\frac{\mathrm{M_{planet}}}{\mathrm{M_{sun}}}} * \mathrm{a}$ where $\mathrm{M_{planet}}$ is the mass of the considered planet and a is the semi-major axis of the precise resonant orbit. Hence we take an approximative relative width of $\frac{\Delta a}{a} = 1\%$ on the semi-major axis to define the area where a planet and a given planetesimal are considered to be in resonance. Then we select all the non-resonant particles that cross the orbit of a planet. The intrinsic collision probability P_i of each of these particles with the planet is computed using the method detailed in Wetherill (1967), implemented in a code developed by Farinella et al. (1992) and kindly provided to us. Once P_i is known for each particle ($i = 1, \ldots, N$), the mass accreted by the planet during the time-step Δt is simply :

$$M_{acc} = \sum_{i=1}^{N} P_i R_{\mathrm{planet}}^2 M_i \Delta t f_{\mathrm{grav}} \qquad (1)$$

where M_i is the mass of the planetesimal (with $\mathrm{M}_i = 0.00349$ Earth mass), and f_{grav} is the gravitational focusing factor. The latter is equal to :

$$f_{grav} = 1 + \frac{V_{\mathrm{lib}}^2}{V_{\mathrm{rel}}^2} \qquad (2)$$

where $V_{\rm rel}$ is the relative velocity between the planet and the planetesimal, and $V_{\rm lib}$ is the escape velocity from the planet. Finally, the total mass accreted by a planet during the full dynamical evolution is simply the sum of M_{acc} over all time-steps taken in the simulation.

3 Results: mass accreted by each giant planets

Fig.1 shows the cumulated mass captured by Jupiter, Saturn, Uranus and Neptune as a function of time in the case of the main simulation. The abrupt increase at 882 Ma is due to the triggering of the LHB when Saturn crosses the 1:2 resonance with Jupiter. It is interesting to notice that this short phase accounts for about two third of the mass acquired by the planets during their full evolution.

Qualitatively, the more massive is the planet, the larger is the massed accreted from the planetesimal disk. This is because larger planets have larger gravitational cross sections.

Uranus and Neptune have comparable masses, and therefore which planets accretes more mass depends on their orbital histories. In the model shown in Fig.1, Uranus first accretes planetesimals at a larger rate than Neptune because Uranus is initially the furthest planet in the system and the closest to the planetesimal disk. However, when the two planets exchange position and Neptune is scattered into the planetesimal disk, it accretes many more planetesimals and eventually exceeds Uranus in terms of total accreted mass. As previously described, the evolution of the system is very chaotic and Fig.1 only represents one of the possible outcomes. In order to assess the variability of the solutions, we also present in Fig.2 the evolution of the 4 "cloned" sim-

ulations focused around the critical period of the 1:2 MMR crossing. We note them 'simu *a*', 'simu *b*', 'simu *c*', and 'simu *d*'. These simulations were started at 868 Myr, just before the 1:2 MMR crossing ($\approx$ 880 Myr), and stopped at 893, 897, 875 and 899 Myr respectively, as soon as the planets reached well separated and relatively stable orbits.

Fig.2 shows that the variability of the accreted masses during that period amounts to up to a factor 2 for all planets except Neptune, for which the variability is a factor 4. The added uncertainty on the results due to the 1 Myr timestep appears small in comparison, as shown by the regularity of the curves.

In order to obtain the evolution of the mass accreted by 4 giant planets during the entire 1.2 Gyr period and to assess the effect of the position switch between Uranus and Neptune on the final accreted mass, we proceed as follows: we simply assume that the planets accreted the same amount of mass as in the main simulation over the first 880 Myr and over the time ranging from the end of each cloned simulation up to 1,200 Myr. In the cases in which Uranus and Neptune do not switch positions, we consider that Uranus accreted before the LHB the same mass accreted by "Neptune" (the 4th planet) in the main simulation, and inversely for Neptune. The results are shown in Fig. 3. We can see that the results for simulations are very similar to the result for the main simulation. However in the simulation *a*, Neptune eventually accretes less mass than Uranus. Conversely, the results for the simulations *b* and *d* are qualitatively different. Neptune is initially the closest planet to the disk and hence accretes much more planetesimals than Uranus also before the LHB. This remains the case during/after the LHB, since Neptune is scattered into the disk and acquires even more planetesimals compared to Uranus.

Table 1 summarizes the total masses accreted by the planets, and compares

them to the masses of heavy elements in their hydrogen-helium envelopes estimated from interior models fitting the giant planets gravitational moments (see Guillot, 2005). As before, for Uranus and Neptune, we separate the cases in which these planets exchange their positions from the cases in which they do not.

In the first case, Uranus accretes an amount of planetesimals comparable to Neptune's, whereas when the order of the ice giants is not switched, Neptune accretes twice more planetesimals than Uranus. In all cases, the masses accreted are significantly smaller than the masses of the envelopes.

For Jupiter and Saturn, the mass accreted is much lower ($\approx 10^{-3}$ times smaller), whereas this ratio can increase to $\sim 7 \times 10^{-2}$ for Uranus and Neptune. Therefore in the framework of the 'Nice' model, the LHB has a stronger impact in terms of heavy elements supply relatively to the envelope mass, in the case of the two latter planets, Uranus and Neptune.

4 Calculation of the envelope enrichments

4.1 Fully mixed case

Once we calculated the mass that each planet accreted during this period, it is straightforward to infer the corresponding change in composition. We thus calculate the increase of the atmosphere's enrichment $\Delta\mathcal{E}$, defined as the amount of heavy elements for a given mass of atmosphere compared to that same value in the Sun. More specifically, the global enrichment increase of a giant planet envelope of mass $M_{\rm envelope}$ accreting a mass of planetesimals

227 $M_{\rm accreted}$ (assuming that planetesimals don't reach the core) is:

228 $$\Delta\mathcal{E}_{\rm LHB} = \frac{M_{\rm accreted}}{M_{\rm envelope} \times Z_{\odot}} \quad (3)$$

229 where $Z_{\odot}$ is the mass fraction of heavy elements in the Sun. Following Grevesse
230 et al. (2005), we use in mean $Z_{\odot} = 0.015$. This global enrichment is also the en-
231 richment of the atmosphere, provided the envelope is well-mixed, a reasonnable
232 assumption given the fact that these planets should be mostly convective (see
233 e.g. Guillot, 2005). These values of enrichment are calculated by taking the
234 mean of the accreted masses of the table 1, and the uncertainty on the enve-
235 lope mass is taken into account. Table 2 shows that this yields relatively small
236 enrichments: the contribution of this late veneer of planetesimals accounts for
237 only about 1% of the total enrichments of Jupiter and Saturn, and up to 10%
238 in the case of Uranus and Neptune, owing to their smaller envelopes.

239 *4.2 Incomplete mixing case*

240 Mixing in the envelopes of giant planets is expected to be fast compared to the
241 evolution timescales, and rather complete because these planets are expected
242 to be fully convective (Guillot, 2005). We want to test the possibility, however
243 unlikely, that mixing was not complete, and that the observed atmospheric
244 enrichments were indeed caused by these late impacts of planetesimals.
245 The values of enrichment, in the hypothesis of an incomplete mixing of the
246 envelope, depends on two elements : the extent of mixing of heavy elements in
247 the envelope, but also the penetration depth of planetesimals in the envelope
248 as a function of their size distribution at the time of the LHB.
249 First let us evaluate to what extent the mixing should occur in order to retrieve

the observed enrichments ($\mathcal{E}_{\rm C/H}$ in Table 2). Following Eq.3, we evaluate the mass of envelope over which planetesimals should penetrate and be mixed to explain the observations :

$$\mathrm{M_{mixed}} = \frac{\mathrm{M_{accreted}}}{\mathcal{E}_{\rm C/H} \times \mathcal{Z}_{\odot}} \tag{4}$$

Using hydrostatic balance, and assuming a constant adiabatic gradient of 0.3, a pressure of 1 bar at the top of the atmosphere and a gravitational acceleration constant and equal to its value at the top of the atmosphere, we calculate the corresponding penetration depth, $\mathrm{h_{mixed}}$, and pressure, $\mathrm{P_{mixed}}$, at this depth . We now have to consider in addition the penetration depth of planetesimals in the envelope as a function of their size distribution at the time of the LHB. The reason is that, even if we could define the extents of penetration and mixing giving the observed enrichments, an important fraction of planetesimals penetrating more deeply in the envelope would anyway cause a heavy elements supply over a larger extent, implying atmospheric enrichments lower than those observed.

We thus have to determine the mass of the envelope shell enriched by a planetesimal of a given size. The main assumption here is to consider that during its entry into the atmosphere, the planetesimal desintegrates and mixes completely with the atmosphere after crossing a mass of gas column equal to its own mass. Thanks to a parallel plane approximation of the atmosphere, the mass of the atmospheric shell thus enriched can be inferred from the ratio between the planetary area $a_{\rm planet}$ and the planetesimal section $a_{\rm pl}$ multiplied by the mass of the considered planetesimal M_{pl} :

$$M_{\rm enriched\ shell} = M_{\rm pl}\frac{a_{\rm planet}}{a_{\rm pl}} \tag{5}$$

We now define $s_{\rm mixed}$, the critical planetesimal radius for which $M_{\rm enriched\ shell} = M_{\rm mixed}$. Following Equations 5 and 6 and considering ice spherical planetesimals with a mass density noted ρ :

$$s_{\rm mixed} = \frac{3 \times M_{\rm mixed}}{4 \times a_{\rm planet} \times \rho} \tag{6}$$

All the planetesimals larger than $s_{\rm mixed}$ will penetrate more deeply than the extent of mixing and will enrich a larger part of the envelope, yielding the enrichments lower than observed.

We now evaluate the mass fraction of planetesimals with sizes larger than $s_{\rm mixed}$. For that we use a bi-modal size distribution inspired from the observations of Trans-Neptunian Bodies (Bernstein et al., 2004), and used successfully by Charnoz and Morbidelli (2007) to explain the number of comets in the scattered disk and the Oort cloud :

$$\frac{dN}{ds} = f_{small} \times s^{-3.5} \qquad s < s_0 \tag{7}$$

$$\frac{dN}{ds} = f_{big} \times s^{-4.5} \qquad s > s_0 \tag{8}$$

with $50km < s_0 < 100km$ the turnover radius, and $f_{\rm small}$ and $f_{\rm big}$ the normalisation factors which depends on the value of s_0 and the total mass of the planetesimals disk (Gomes et al., 2005). For each planet, the mass fraction is calculated with s_0=50 and 100 km in order to have a good range of values around the estimated one which is approximately 70 km according to Fuentes and Holman (2008).

Table 3 summarizes the results obtained in the case of an incomplete mixing. Compared to the whole envelope mass, the masses of layer enriched by this incomplete mixing are of the order of 1% for Jupiter and Saturn, and between

5 and 10% for Uranus and Neptune. As previoulsy mentioned, these values and those of the related quantities are a priori unrealistic because of the globally convective structure of the giant planets. Moreover, according to the results of mass fraction in Table 3, we see that the large planetesimals with a size bigger than s_{mixed} are comparable and even predominant in terms of mass compared to the small ones, especially for Uranus and Neptune.

Therefore even if we assume an incomplete mixing giving the observed enrichments, the important supply of heavy elements by the large planetesimals at layers deeper than $\mathrm{h_{mixed}}$ will imply anyway lower enrichments than those observed.

In summary, it appears that the observed enrichments cannot be explained in the context of the Late Heavy Bombardment even by using the hypothesis of an incomplete mixing.

5 Conclusion

In this work, we evaluated the extent to which the late heavy bombardment could explain the observed enrichments of giant planets.

We calculated the mass accreted by each planet during this period thanks to several dynamical simulations of the LHB within the so-called "Nice" model. The accreted masses were found to be much smaller than those of the envelopes of each giant planet. In the realistic hypothesis of a global mixing in these envelopes, we found the enrichments over the solar value to be approximately two orders of magnitude smaller than the observations for Jupiter and Saturn and one order of magnitude smaller than the observations for Uranus and Neptune.

We then tested the possibility of an incomplete mixing in the giant planets envelopes to account for the observed enrichments. With a size distribution of planetesimals inferred from observations of trans-neptunian bodies, we found that the enrichments were always at least a factor of 2 lower than observed. Given the efficient convection expected in the deep atmosphere, we expect however the mixing to be complete.

Therefore we conclude that the enriched atmospheres of the giant planets do not result from the Nice model of the LHB and probably from any model describing the LHB. In fact Guillot and Gladman (2000)'s calculations showed that the mass needed to explain Jupiter's and Saturn's enrichments would be certainly much too large, in any late heavy bombardment model. Earlier events should thus be invoked in the explanation of the enriched atmopspheres of giant planets. On the other hand the enrichment process during the LHB may not be completely negligeable when considering fine measurements of the compositions of giant planets (eg. Marty et al., 2008). When present it may also have a role in enriching the envelopes of close-in extrasolar giant planets because of their radiative structure.

We acknowledge support from the Programme National de Planétologie. We thank one of the referees, Brett Gladman, for comments that improved the article.

References

Alibert, Y., Mordasini, C., Benz, W., Winisdoerffer, C., Apr. 2005. Models of

giant planet formation with migration and disc evolution. A&A 434, 343–353.

Bernstein, G. M., Trilling, D. E., Allen, R. L., Brown, M. E., Holman, M., Malhotra, R., Sep. 2004. The Size Distribution of Trans-Neptunian Bodies. AJ 128, 1364–1390.

Charnoz, S., Morbidelli, A., Jun. 2007. Coupling dynamical and collisional evolution of small bodies. Icarus 188, 468–480.

Farinella, P., Davis, D. R., Paolicchi, P., Cellino, A., Zappala, V., Jan. 1992. Asteroid collisional evolution - an integrated model for the evolution of asteroid rotation rates. A&A 253, 604–614.

Flasar, F. M., Achterberg, R. K., Conrath, B. J., Pearl, J. C., Bjoraker, G. L., Jennings, D. E., Romani, P. N., Simon-Miller, A. A., Kunde, V. G., Nixon, C. A., Bézard, B., Orton, G. S., Spilker, L. J., Spencer, J. R., Irwin, P. G. J., Teanby, N. A., Owen, T. C., Brasunas, J., Segura, M. E., Carlson, R. C., Mamoutkine, A., Gierasch, P. J., Schinder, P. J., Showalter, M. R., Ferrari, C., Barucci, A., Courtin, R., Coustenis, A., Fouchet, T., Gautier, D., Lellouch, E., Marten, A., Prangé, R., Strobel, D. F., Calcutt, S. B., Read, P. L., Taylor, F. W., Bowles, N., Samuelson, R. E., Abbas, M. M., Raulin, F., Ade, P., Edgington, S., Pilorz, S., Wallis, B., Wishnow, E. H., Feb. 2005. Temperatures, Winds, and Composition in the Saturnian System. Science 307, 1247–1251.

Fuentes, C. I., Holman, M. J., Jul. 2008. a SUBARU Archival Search for Faint Trans-Neptunian Objects. AJ 136, 83–97.

Garaud, P., Dec. 2007. Growth and Migration of Solids in Evolving Protostellar Disks. I. Methods and Analytical Tests. APJ 671, 2091–2114.

Gomes, R., Levison, H. F., Tsiganis, K., Morbidelli, A., May 2005. Origin of the cataclysmic Late Heavy Bombardment period of the terrestrial planets.

372 Nature 435, 466–469.
373 Grevesse, N., Asplund, M., Sauval, A. J., 2005. The New Solar Chemical Com-
374 position. In: Alecian, G., Richard, O., Vauclair, S. (Eds.), EAS Publications
375 Series. Vol. 17 of Engineering and Science. pp. 21–30.
376 Guillot, T., Jan. 2005. THE INTERIORS OF GIANT PLANETS: Models and
377 Outstanding Questions. Annual Review of Earth and Planetary Sciences 33,
378 493–530.
379 Guillot, T., Gautier, D., 2007. Giant planets. Treatise on Geophysics, Vol. 10,
380 Planets and Moons, Elsevier, pp. 439–464.
381 Guillot, T., Gladman, B., 2000. Late Planetesimal Delivery and the Composi-
382 tion of Giant Planets (Invited Review). In: Garzón, G., Eiroa, C., de Winter,
383 D., Mahoney, T. J. (Eds.), Disks, Planetesimals, and Planets. Vol. 219 of
384 Astronomical Society of the Pacific Conference Series. pp. 475–+.
385 Guillot, T., Hueso, R., Mar. 2006. The composition of Jupiter: sign of a (rela-
386 tively) late formation in a chemically evolved protosolar disc. MNRAS 367,
387 L47–L51.
388 Guillot, T., Stevenson, D. J., Hubbard, W. B., Saumon, D., 2004. The interior
389 of Jupiter. Jupiter. The Planet, Satellites and Magnetosphere, pp. 35–57.
390 Ida, S., Guillot, T., Morbidelli, A., Oct. 2008. Accretion and Destruction of
391 Planetesimals in Turbulent Disks. APJ 686, 1292–1301.
392 Ida, S., Lin, D. N. C., Mar. 2004. Toward a Deterministic Model of Planetary
393 Formation. I. A Desert in the Mass and Semimajor Axis Distributions of
394 Extrasolar Planets. APJ 604, 388–413.
395 Levison, H. F., Morbidelli, A., Vanlaerhoven, C., Gomes, R., Tsiganis, K.,
396 Jul. 2008. Origin of the structure of the Kuiper belt during a dynamical
397 instability in the orbits of Uranus and Neptune. Icarus 196, 258–273.
398 Lodders, K., Jul. 2003. Solar System Abundances and Condensation Temper-

399 atures of the Elements. ApJ 591, 1220–1247.

400 Marty, B., Guillot, T., Coustenis, A., Achilleos, N., Alibert, Y., Asmar, S.,
401 Atkinson, D., Atreya, S., Babasides, G., Baines, K., Balint, T., Banfield, D.,
402 Barber, S., Bézard, B., Bjoraker, G. L., Blanc, M., Bolton, S., Chanover, N.,
403 Charnoz, S., Chassefière, E., Colwell, J. E., Deangelis, E., Dougherty, M.,
404 Drossart, P., Flasar, F. M., Fouchet, T., Frampton, R., Franchi, I., Gau-
405 tier, D., Gurvits, L., Hueso, R., Kazeminejad, B., Krimigis, T., Jambon,
406 A., Jones, G., Langevin, Y., Leese, M., Lellouch, E., Lunine, J., Milillo,
407 A., Mahaffy, P., Mauk, B., Morse, A., Moreira, M., Moussas, X., Murray,
408 C., Mueller-Wodarg, I., Owen, T. C., Pogrebenko, S., Prangé, R., Read,
409 P., Sanchez-Lavega, A., Sarda, P., Stam, D., Tinetti, G., Zarka, P., Zar-
410 necki, J., Schmidt, J., Salo, H., Aug. 2008. Kronos: exploring the depths of
411 Saturn with probes and remote sensing through an international mission.
412 Experimental Astronomy, 34–+.

413 Morbidelli, A., Levison, H. F., Gomes, R., 2008. The Dynamical Structure
414 of the Kuiper Belt and Its Primordial Origin. The Solar System Beyond
415 Neptune, pp. 275–292.

416 Morbidelli, A., Levison, H. F., Tsiganis, K., Gomes, R., May 2005. Chaotic
417 capture of Jupiter's Trojan asteroids in the early Solar System. Nature 435,
418 462–465.

419 Nesvorný, D., Vokrouhlický, D., Morbidelli, A., May 2007. Capture of Irregular
420 Satellites during Planetary Encounters. AJ 133, 1962–1976.

421 Owen, T., Mahaffy, P., Niemann, H. B., Atreya, S., Donahue, T., Bar-Nun,
422 A., de Pater, I., Nov. 1999. A low-temperature origin for the planetesimals
423 that formed Jupiter. Nature 402, 269–270.

424 Paardekooper, S.-J., Jan. 2007. Dust accretion onto high-mass planets. A&A
425 462, 355–369.

426 Saumon, D., Guillot, T., Jul. 2004. Shock Compression of Deuterium and the
427 Interiors of Jupiter and Saturn. ApJ 609, 1170–1180.
428 Tsiganis, K., Gomes, R., Morbidelli, A., Levison, H. F., May 2005. Origin of
429 the orbital architecture of the giant planets of the Solar System. Nature
430 435, 459–461.
431 Wetherill, G. W., 1967. Collisions in the asteroid belt. JGR 72, 2429–2444.
432 Wong, M. H., Mahaffy, P. R., Atreya, S. K., Niemann, H. B., Owen, T. C., Sep.
433 2004. Updated Galileo probe mass spectrometer measurements of carbon,
434 oxygen, nitrogen, and sulfur on Jupiter. Icarus 171, 153–170.

435 Caption figure 1 : Mass accreted (in Earth mass units) by Jupiter (plain),
436 Saturn (dashed), Uranus (dash-dotted) and Neptune (dotted) respectively, as
437 a function of time (in years). The simulation corresponds to the main simula-
438 tion described in the text, in which Uranus and Neptune switch their relative
439 positions.

440 caption figure 2 : Additional mass accreted (in Earth mass units) during the
441 time range of the 4 'cloned' simulations. Figures a and c (left) correspond
442 to the cases in which Uranus and Neptune exchange position at the time of
443 the LHB. Figures b and d (right) show the result of simulations in which the
444 four planets preserve their initial order. These 'cloned' simulations start 868
445 Myr after the beginning of the planets migration and are stopped once giant
446 planets acquired well separated and stable orbits.

447 Caption figure 3 : Mass accreted(in Earth mass units) for the 4 'cloned' sim-
448 ulations during the whole time scale of the 'Nice' model. In each of these four
449 panels, the period before 868 Myr and after 875-899 Myr (depending on the
450 simulation) is assumed to be identical to the main simulation. Figures a and c

(left) correspond to the cases in which Uranus and Neptune exchange position at the time of the LHB. Figures b and d (right) show the result of simulations in which the four planets preserve their initial order.

Caption table 1 : Planetesimal masses accreted by the giant planets after the disappearance of the protosolar gaseous disk.

Caption table 2 : Enrichment increase (see equation 3) calculated from the different simulations of the model. The values of the observed $\epsilon_{C/H}$ are derived from Guillot (2005).

Caption table 3 : Mass of enriched layer, extent of mixing h_{mixed}, pressure level at the bottom of the mixing area P_{mixed}, and planetesimal radii s_{mixed}, which would match the observed enrichments. The last column is the mass percentage corresponding to the planetesimals whose the radius is larger than s_{mixed}, the range being due to the two limiting values of s_0 used.

Fig. 1.

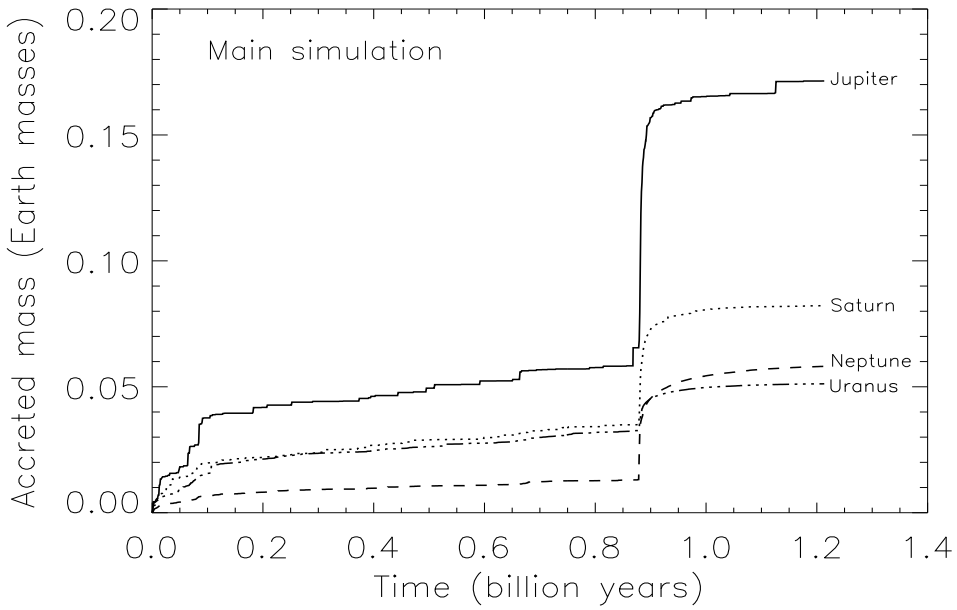

Fig. 2.

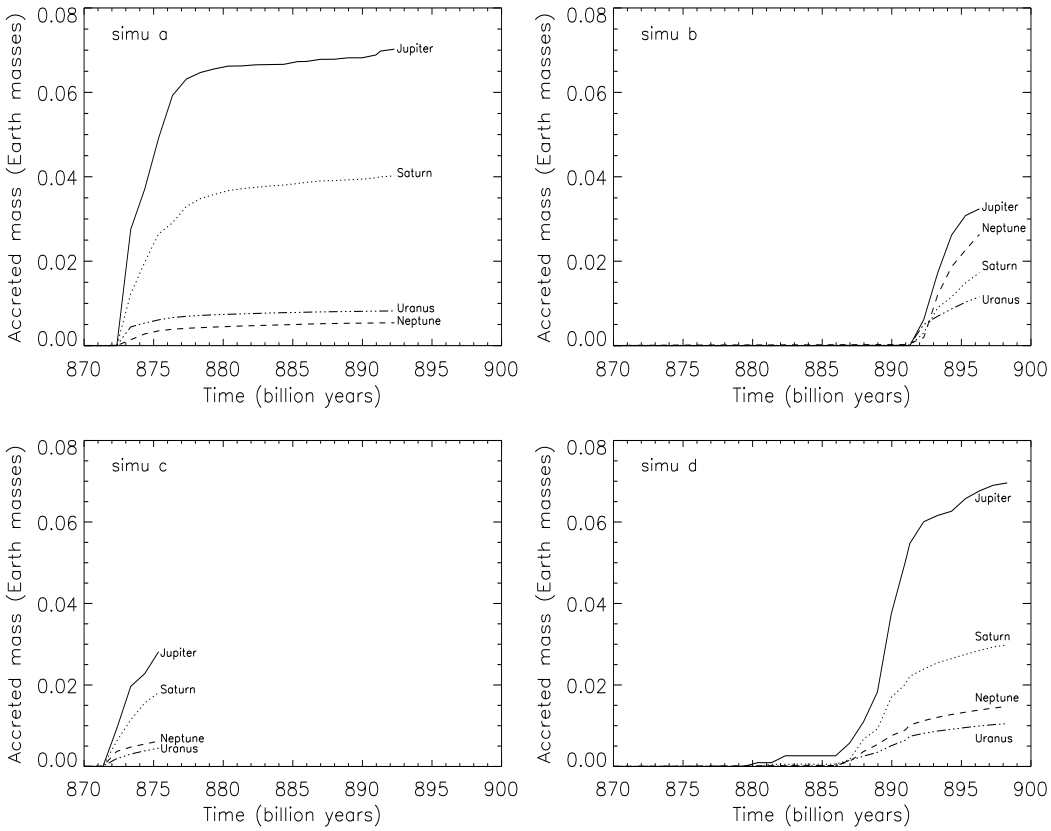

Table 1

Giant planet	*Envelope mass* [$M_\oplus$]	*Accreted mass* [$M_\oplus$]
Jupiter	$300 - 318$	$0.11 - 0.20$
Saturn	$70 - 85$	$0.06 - 0.10$
Uranus (w/ inversion)	$1 - 4$	$0.048 - 0.055$
(w/o inversion)		$0.029 - 0.031$
Neptune (w/ inversion)	$1 - 4$	$0.033 - 0.064$
(w/o inversion)		$0.060 - 0.072$

Fig. 3.

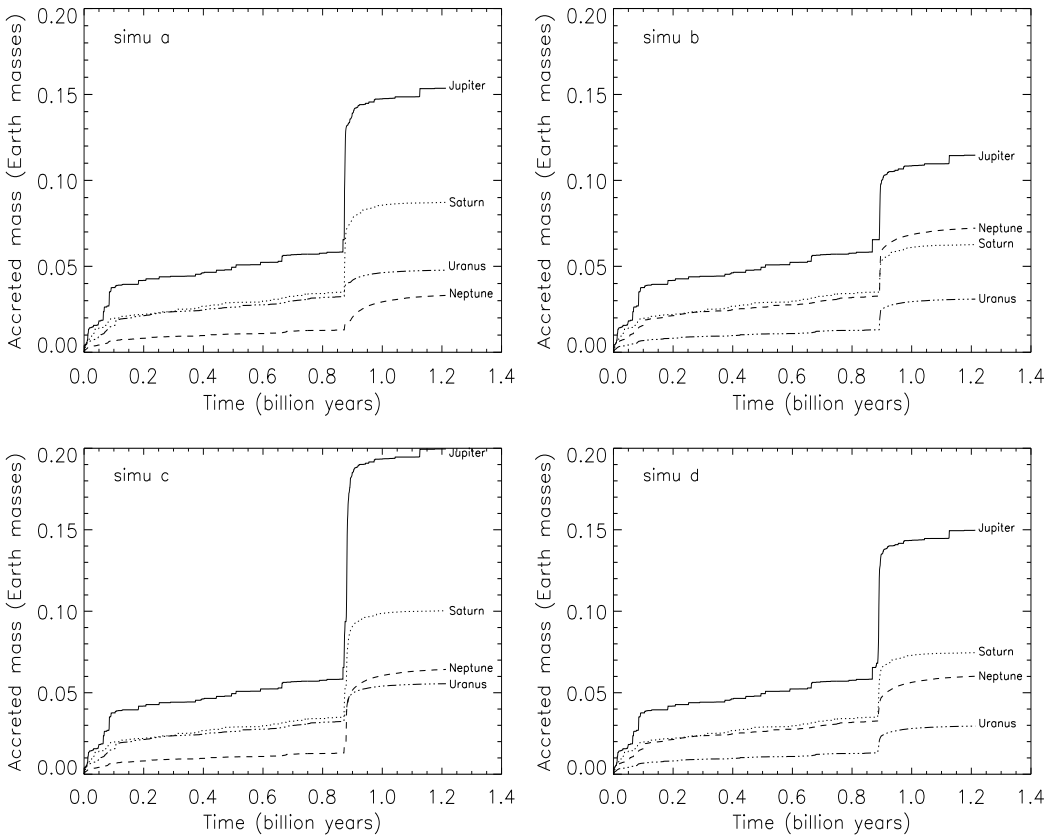

Table 2

Giant planet	$\Delta\varepsilon_{\rm LHB}$	*Observed* $\varepsilon_{\rm C/H}$
Jupiter	0.032-0.034	4.1 ± 1
Saturn	0.062-0.076	7.4 ± 1.7
Uranus (w/ inversion)	0.8 – 3.4	45 ± 20
(w/o inversion)	0.5 – 2	
Neptune (w/ inversion)	0.8-3.2	45 ± 20
(w/o inversion)	1.1-4.4	

Table 3

Giant planet	M_{mixed} ($M_\oplus$)	h_{mixed} (km)	P_{mixed} (bar)	s_{mixed} (km)	% $M(s > s_{mixed})$
Jupiter	3.41	2000	48300	248	23%-32%
Saturn	0.82	2200	7200	86	39%-54%
Uranus (w/ inversion)	0.11	1200	4200	63	44%-60%
(w/o inversion)	0.07	1000	2500	37	57%-69%
Neptune (w/ inversion)	0.11	1000	5100	61	45%-61%
(w/o inversion)	0.15	1400	13100	84	39%-54%